Willem 3D: Reprocessed, inverted, revitalized

Mark Sams[1], Shane Westlake[2], Josh Thorp[3], and Ebrahim Zadeh[1]

Abstract

The Carnarvon Basin on the North West Shelf of Australia is a world-class hydrocarbon province, with the pace of discoveries significantly accelerating in the last 15 years. The high success rate has been aided by improvements in seismic data quality, hydrocarbon detection techniques, and widespread 3D seismic surveys. This has led to the identification of several new play concepts, an increase in target depths, and an extension into more difficult seismic data areas. New broadband acquisition technologies undoubtedly have delivered a significant enhancement in many parts of the basin, but there is still much to be gained from existing 3D seismic data sets. Broadband seismic data reprocessing, prestack depth migration, and facies-based seismic inversion can offer a cost-efficient exploration tool to maintain the historical success rates. The open-file Willem 3D seismic survey adjacent to the giant Io/Jansz, Wheatstone, and Pluto gas fields is located in an area that has been explored insufficiently. The 2006 seismic data originally were regarded to be of good quality, but with advancements in acquisition and reprocessing techniques, the imaging result is now considered to be poor relative to modern-day seismic data sets. The Urania-1 gas discovery and northern extent of the Pluto field were detected on the original data, but other prospects based on this data set proved to be unsuccessful. The complex overlying Tertiary channels and the presence of shallow strong seismic attenuation caused historical data-imaging limitations. Recent prestack depth-migration reprocessing has improved the data quality, with deghosting providing a significant uplift throughout the processing workflow. A facies-based inversion of the reprocessed data has delineated the known gas accumulations successfully and has predicted the location and dimensions of the recent Woodside Petroleum Pyxis-1 gas discovery.

Introduction

The 2700 km² Willem 3D seismic survey was acquired by Woodside Petroleum in 2006 and is situated in the Carnarvon Basin on the North West Shelf of Australia. To the south are the Pluto and Wheatstone fields, and to the west, adjacent with the survey, is the giant Io/Jansz gas field (Figure 1). Six wells have been drilled within the survey area, from Urania-1 in 2000 until the recent Pyxis-1 gas discovery drilled in 2015 by Woodside Petroleum, although drilling success on the data has had mixed results.

The geologic setting of the Northern Carnarvon Basin (and its deepwater portion, known collectively as the Exmouth Plateau) is the result of multiple periods of extension, minor Upper Triassic compression, subsidence, and minor compression associated with the fragmentation of eastern Gondwana, followed by compression in the uppermost Miocene (Longley et al., 2002; Jablonski and Saitta, 2004). The Archean and Proterozoic structures and Gondwanna plate tectonics controlled the shape of the Paleozoic subasins. As more sediments were deposited, the impact of the global tectonic stresses become more evident within the younger Mesozoic basins,

which superimposed the northeastern-to-southwestern orientation on the preexisting tectonic fabric.

The Willem 3D is in a highly prospective area of the Carnarvon Basin with multiple play and trap configurations (Figure 2). However, historical drilling has focused only on two main play levels: the Upper Triassic fluviodeltaic sandstones of the Mungaroo Formation — e.g., Pluto and Wheatstone fields — and the Oxfordian shallow-marine transgressive sandstones of the Eliassen Formation — e.g., the Io/Jansz field. Recent drilling of the Noblige gas discovery by Woodside Petroleum in the neighboring permit has high-graded an intra-Mungaroo play target, and the recent Pyxis-1 well demonstrates further potential in the Upper Jurassic, likely to
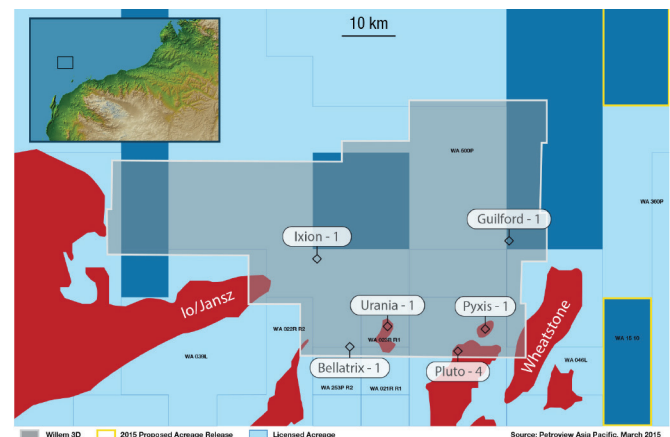
Figure 1. Location map of the Willem 3D seismic survey. The wells within the seismic area are indicated, as are the nearby gas fields and block boundaries. The location of the map with respect to the northwestern coast of Australia is shown in the inset.
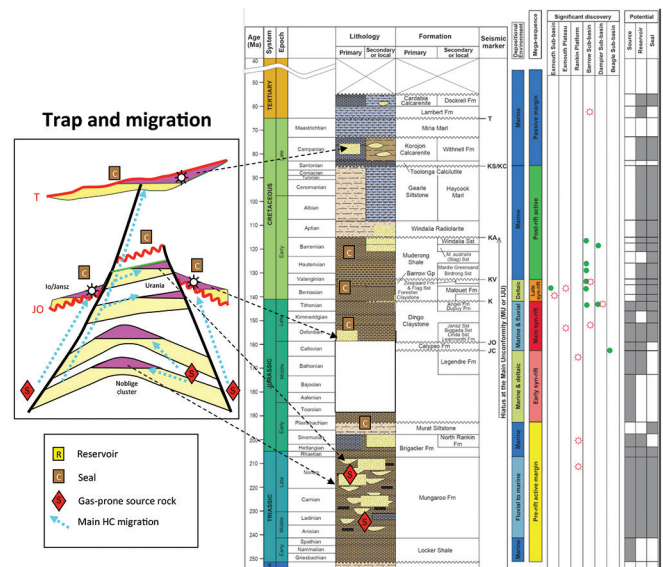
Figure 2. Stratigraphy, plays, trap, and charge configuration in the survey area. Sratigraphic table based on DITR (2007).

[1]Ikon Science.
[2]Finder Exploration Pty. Ltd.
[3]Searcher Seismic Pty. Ltd.

be Tithonian transgressive sandstones. To the north of the survey, the Atlas-1 and Titania-1 wells intersected a Campanian basin-floor fan sandstone that extends updip into the survey. The Guilford-1 well has strong gas shows at an equivalent interval because it tested a breached trap.

Despite a high chance of success driven by 3D seismic data and an AVO-rich area, some wells within the survey failed to encounter hydrocarbons when testing seismic amplitudes that subsequently were found to be caused by the tuning effect on the edge of the local depositional center (e.g., Ixion-1).

The main exploration risks within the survey area are absence of hydrocarbon charge, top-seal leakage, and absence of economically sized structures, given that the water depths are greater than 1000 m for the most part. The aim of reprocessing the data was to target two of these risks, the presence of hydrocarbon charge and top-seal leakage, through a broadband processing workflow and prestack depth migration. The original data quality was acceptable, but improvements even on perceived good-quality data can be significant in both the imaging space and for data inversion, allowing petroleum explorers to reassess areas previously passed over.
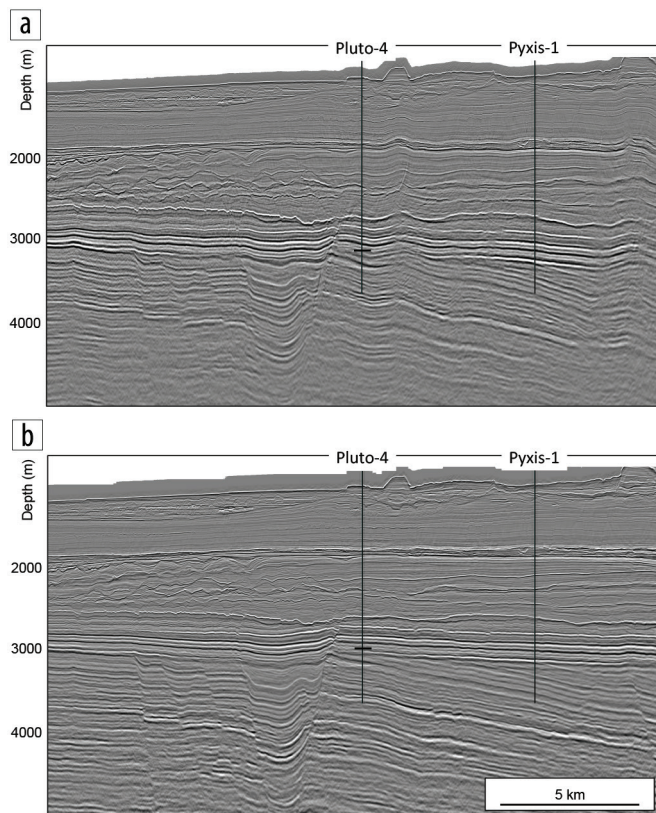
Reprocessing

Figure 3 shows a comparison of the original data and reprocessed data. The comparison highlights a number of issues that have been addressed through the reprocessing. The poor imaging, amplitude attenuation, multiple energy, and signal-to-noise drop below the Cretaceous all have been mitigated to a large degree. The causes of these problems are also clear: the strong bathymetric relief, the complex overburden, and shallow anomalies associated with potential leakage features.

The data had been acquired in 2006 with then-modern equipment and a 5.5 km cable. The processing was a standard PSTM. The limitations of such processing were understood prior to reprocessing, and the reprocessing workflow was designed to address these limitations. Of significance was the use of broadband deghosting that now has become a common tool for conventionally shot streamer data. The deghosting improved the demultiple sequence by having a zero-phase wavelet with minimal side lobes. The surface-related multiple elimination (SRME) worked quite well, and having a better understanding of the phase allowed for a tighter premigration radon. Integrating regional geologic knowledge early improved the initial velocity analysis.

Furthermore, going into the velocity modeling, there was less ambiguity of the events in the overburden, which allowed for significant additional detail in the velocity model. Having reduced tuning effects/constructive interference on the flanks of channels and thin beds, the tomography could define the velocity contrasts accurately and helped to account for the raypath distortion seen on the far offsets of the original data set (Figure 4).

Depth migration consisted of five iterations of constrained global tomography to generate a final velocity model and two anisotropic updates using well control to constrain epsilon and delta. Emphasis was placed on properly resolving the channel features. Resolving the deeper complex features aided in identifying shallow anomalies. The anisotropic model was layer-constrained using regional lithologic knowledge and quality-controlled partly through a focus on the deep AVO response on the far offsets. The detailed interpretation resulted in high-resolution velocity and anisotropy models.

Postmigration, the detailed velocity model allowed for a more effective demultiple because tighter constraints could be applied and the anisotropic imaging ensured a stable offset response for stacking. The data were stacked into partial-angle stacks with angle ranges of 5° to 20° for near, 15° to 30° for mid-, 25° to 40° for far, and 35° to 50° for ultrafar. Prior to inversion, the partial-angle stacks were conditioned further through the removal of random noise, spectral balancing, and residual time alignment. Amplitude compensation via a long-gate automatic gain control (AGC) was applied to counter

Figure 3. Comparison of the full-stack seismic data after (a) original PSTM processing in time then converted to depth and (b) reprocessed PSDM in depth. Significant improvements in imaging have been made through reprocessing, in particular below the Cretaceous (near base Cretaceous marker is shown in the Pluto-4 well). The line passes through the Pluto well in the center of the cross section, and a fluid contact, flat in depth, can be interpreted.
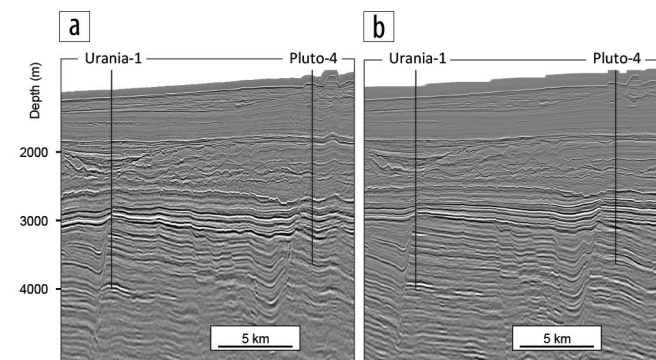
Figure 4. Comparison of the far-stack seismic data after (a) original PSTM processing in time then converted to depth and (b) reprocessed PSDM in depth. Distortions of the far-stack events in the original data are highlighted by the flat spots seen at Urania-1 and Pluto-4 in the reprocessed data that are not flat in time or in depth on the original data.

the effects of dimming in the fault shadows and residual attenuation from shallow features. Although AGC normally is not considered a suitable process prior to seismic inversion, in this case, the benefits of detecting gas in the fault shadows at Urania-1 and Pluto-4 were greater than any observed detrimental effect.

Inversion

Inversion was carried out to improve the interpretability of the seismic data. The type of inversion chosen was a facies-based simultaneous inversion (Kemper and Gunning, 2014). That is, the partial-angle-stack seismic data are inverted simultaneously to elastic rock properties and a most likely facies model.

There are several reasons for selecting such an inversion. First, simultaneous inversion combines the well-known benefits of inversion with the AVO in the seismic to produce at least acoustic and shear impedance models of the subsurface, which when combined allow for a better definition of lithologies and fluids. Second, combining simultaneous inversion with a facies inversion removes the requirement for an initial low-frequency model and introduces constraints that potentially improve the definition of thin and thick beds. The lack of a requirement for a low-frequency model is important in this case because there is limited well control within a large geographic area. The simple interpolation/extrapolation of a few wells across such a large area would be meaningless. Instead, by including facies within the inversion, all that is required is to define time-dependent rock-physics relationships for each of the chosen facies, complete with an assessment of uncertainty.

Note that the trends are developed in time as the seismic data are inverted in the time domain. Of course, the assumption is that these rock-physics models are applicable over the entire area and can be extrapolated to depths greater than the well control. The low-frequency components of the resulting absolute elastic-property models are determined by the predicted distribution of facies and the depth trends associated with those facies.

The inputs for the inversion include partial-angle stacks and associated wavelets, estimates of the noise in the partial-angle stacks, facies definition and depth-dependent rock-physics models with uncertainties for each facies, and global prior probabilities of each facies within defined stratigraphic intervals. These inputs require well data. Five wells were available with open-file data: Ixion-1, Bellatrix-1, Urania-1, Pluto-4, and Guilford-1 (see Figure 1 for locations). Only two of these wells, Bellatrix-1 and Urania-1, had complete sets of elastic logs (P-sonic, S-sonic, and density). No petrophysical interpretations were available, and because of time constraints, none was carried out.

The choice of what facies to invert for was based on the lithologies and fluids present, their relevance to a geologic interpretation, and their separation in the elastic domain. A facies-based inversion aims to use the seismic data to constrain the distribution of the facies, and so the facies must have some degree of separation in the elastic domain and particularly in terms of acoustic and shear impedance. Such a definition might not be compatible with an idealized geologic definition. Thus, some compromise must be made, and often the number of facies is limited by the degree of overlap in the elastic domain. As such, these facies should be termed elastofacies. In this case, five facies were defined and interpreted in each well based on well reports and the responses of several logs, including GR, resistivity, PEF, P-sonic, and density. The facies selected were shale, marl, limestone, brine sand, and gas sand (Figure 5).

The rock-physics model for each of the facies is defined by a depth trend (converted to time with a background velocity model) in terms of P-velocity and the relationship between P-velocity and S-velocity and between P-velocity and density (Figure 6). Each component of the model has associated uncertainties. The rock-physics models therefore represent time-varying three-dimensional probability density functions. The relationships in this case were defined from the upscaled in situ data and therefore were controlled completely by the two wells that included the measured S-sonic data. The depth trends are related to a datum. The optimal datum was found to be the top of the Cretaceous, and an associated horizon was available to act as the datum during inversion. It should be noted that Bellatrix-1 is a relatively shallow well in which the majority of rocks are either marl or limestone. The only gas sands with measured S-sonic are in the Urania-1 well.

A wavelet was estimated for each partial-angle stack using the Bellatrix-1 and Urania-1 wells, which have S-sonic available (Figure 7). The uncertainty in the wavelet estimates was used as a starting point for the noise assigned to each of the stacks. The amount of noise, the uncertainties in the rock-physics relationships, and the prior probabilities for each of the facies were updated during the testing of the inversion until acceptable results were obtained. The prior probabilities were adjusted within several stratigraphic units defined by interpreted horizons. The optimization of the input variables was made through the prediction of the facies at all the wells and the assessment of the facies distribution away from well control based on geologic expectation.
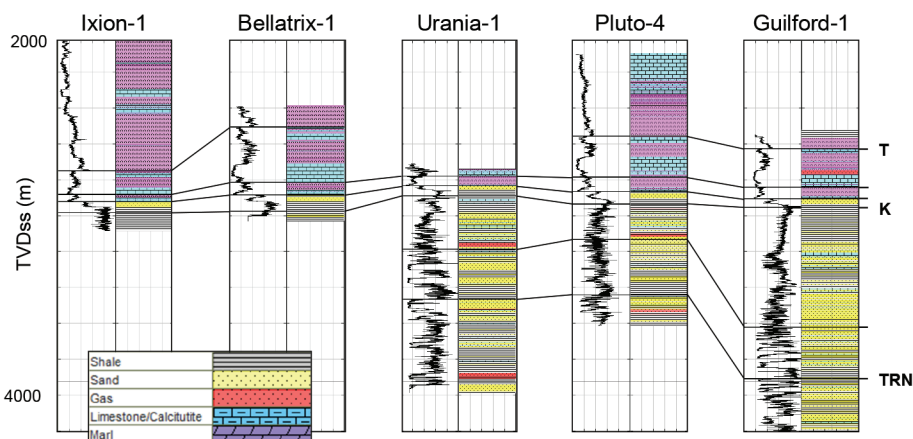
Figure 5. The elastofacies have been defined in each well. The figure shows the wells in TVDss, with the facies displayed alongside the gamma-ray curves (scaled at 0 to 200 API). Correlations have been drawn where information is present from well reports. Note that gas is indicated at two levels in Urania-1 and two levels in Pluto-4, although the lower gas sand has high water saturations, and at one level in the Cretaceous in Guilford-1. The named markers represent base Tertiary (T), near base Cretaceous (K), and top Triassic (TRN).
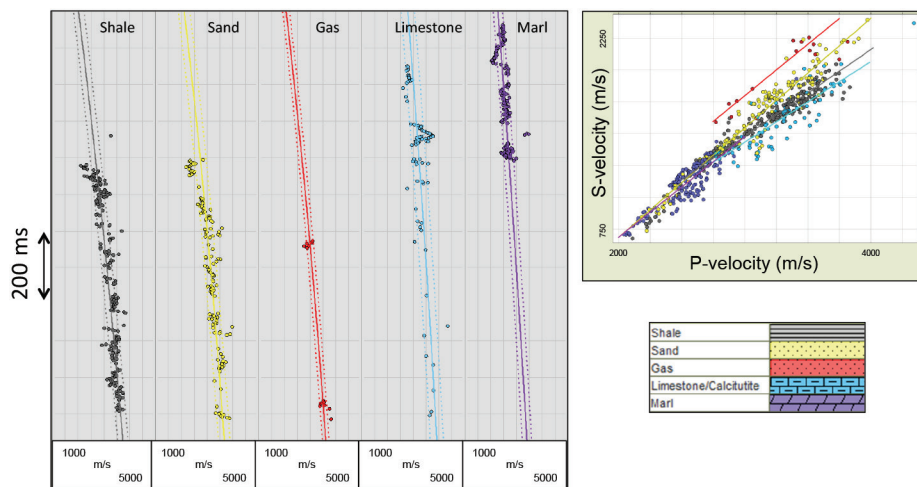
In the case of Urania-1, quality control is available for facies and elastic properties. Figure 7 shows a typical quality-control panel. The predicted facies can be compared with the facies defined in the wells, the predicted elastic properties can be compared with the measured elastic properties, and the seismic can be compared with the synthetic for each angle stack.

In terms of the elastic properties, both the relative and absolute properties can be compared. The lowest frequencies below the seismic data limit do not come from a low-frequency model, as is the case for a standard simultaneous inversion. Instead, they are determined by the inverted vertical facies distribution and the time-trend model for each facies. Because the time trends are derived from the well data, the lowest frequencies will be correct if the facies are predicted well. For the Urania-1 shown in Figure 8, there is a good fit to the absolute and relative elastic properties and a reasonable fit to the facies. In particular, the two gas sands are predicted well.

Results

The results can be assessed by the conformity of the facies distribution to geologic expectation and to the match at all the wells. Given that the rock-physics models were based on only the two wells where S-sonic was measured, the prediction of facies, and in particular gas sand, in the other wells is of keen interest when assessing the confidence in the prediction of the facies elsewhere in the volume. In Figure 9, the predicted lithology is compared against all the wells. There is a high correlation. It is interesting to note that although no Cretaceous gas sands were available for input into the rock-physics model, the

Figure 6. The measured P-velocity well data are plotted in two-way time below a chosen datum. An exponential trend is fitted to the data for each facies, and an uncertainty estimate is made (solid and dashed lines, respectively). Linear relationships are derived between P-velocity and S-velocity and uncertainties estimated (not shown). Linear relationships and uncertainties also are developed between P-velocity and density (not shown). Note: Only Bellatrix-1 and Urania-1 were used for this analysis.
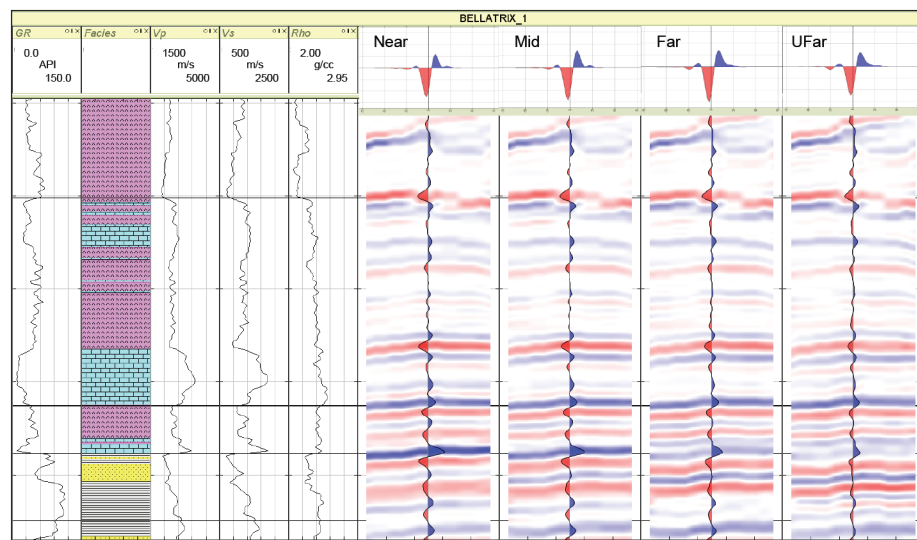

Figure 7. The Bellatrix well was used for estimating the wavelets because it provided the better tie compared with Urania-1. GR, facies, P-velocity, S-velocity, and density logs are shown on the left. Seismic panels show the conditioned seismic along a short section through the well location. The estimated wavelet is shown at the top, and the synthetic is shown as a single wiggle trace.

prediction of the gas sand in the Guilford-1 well is accurate. It is also interesting to note that in the two wells where no gas sands were encountered, the inversion predicts that there are no gas sands.

The Pyxis-1 discovery by Woodside Petroleum was announced a short time before the inversion part of the project was initiated. Only the well location and the fact that gas had been discovered were known; neither the depth nor the stratigraphic level of the find was known. A gas sand was predicted at the Pyxis-1 well location within the Upper Jurassic, possibly Tithonian interval. The discovery is of significant size, covering an area of approximately 20 km², and the inversion has provided a clear definition of the dimensions, including the prediction of a thin

gas leg separated from the main accumulation by a small graben (Figure 10). The inversion predicts a gas-bearing sand with a thickness of approximately 60 ft at the well location, which compares favorably with the 64 ft announced by Woodside Petroleum. It is interesting to note that the inversion predicts gas below the TD of the Pyxis-1 well at stratigraphic levels similar to those at Pluto and Urania, where gas is known to exist.

Conclusions

Open-file seismic and well data have been used to provide a highly improved model of an area of significant interest in the Carnarvon Basin on the North West Shelf of Australia. Three-dimensional seismic data were reprocessed, and by using modern
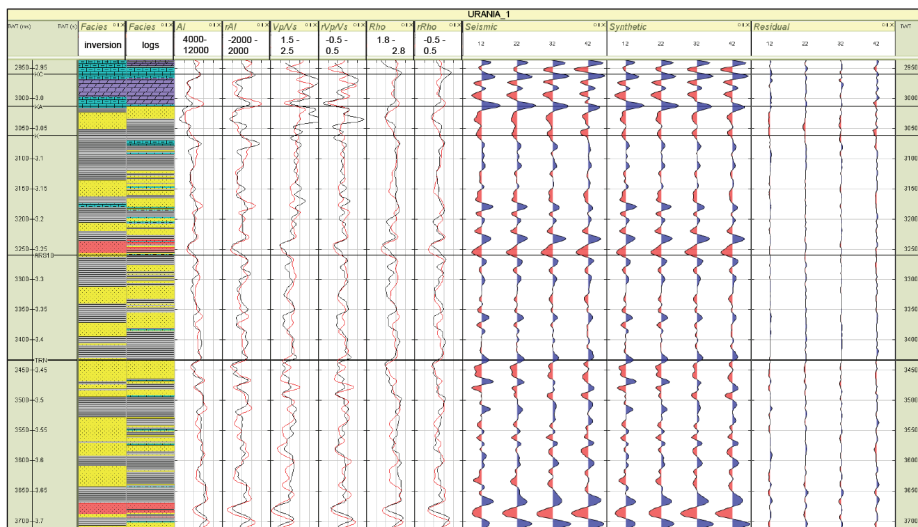
Figure 8. The inversion parameters are optimized at first by inverting at the well locations. The quality-control panel shows (from left) a comparison of inverted and well facies; elastic logs of acoustic impedance, V_P/V_S, and density from inversion in red and from the well in black (these comparisons are shown as absolute and relative properties); seismic-angle traces, synthetics from inversion, and residuals. The elastic logs have been high-cut-filtered to the upper seismic limit for the absolute and band-pass-filtered to the seismic bandwidth for the relative properties. Note that unlike standard deterministic inversions, the absolute predictions are not constrained by an initial low-frequency model and so represent true predictions for all frequencies present.
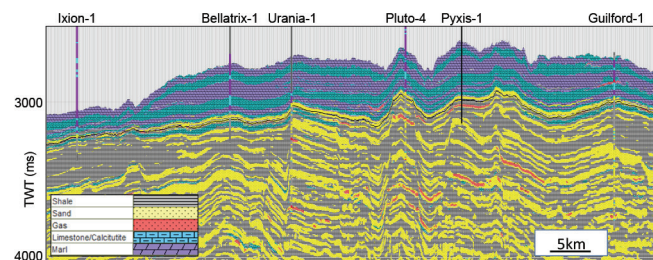
Figure 9. The inversion predicts elastic properties and the most likely facies. The inverted facies are shown along a traverse that passes through each of the wells. The predictions at the wells are reasonable. In terms of gas, the inversion predicts the two gas sands in Urania-1, the upper gas sand in Pluto-4, and the shallow Cretaceous gas sand in Guilford-1.
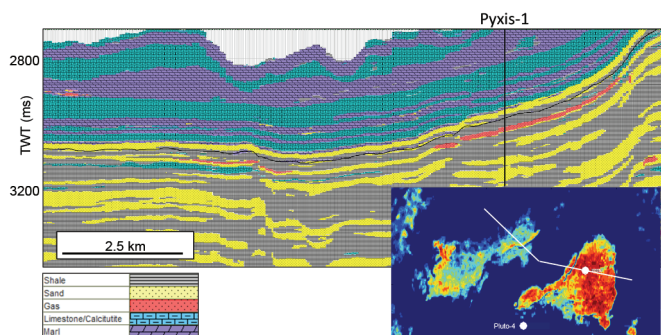
Figure 10. The inversion predicts the presence of a gas sand just below the near base Cretaceous (K) horizon. The thickness of the sand has been calculated and represents about 60 ft at the Pyxis well location, which compares favorably with the 64 ft announced by Woodside. A thinner accumulation is predicted to occur to the west on the other side of a small graben. To the east, the hydrocarbons appear to be trapped by a fault because the sand continues beyond the edge of the gas.

techniques — in particular, broadband deghosting — and with attention to detail, a markedly improved image was produced, optimized for quantitative interpretation. Well data were used to provide a depth-dependent rock-physics model that was used within a facies-based inversion. Despite the limited control provided by data from just two wells, the prediction of facies by comparison with three other wells at various levels provides significant confidence in predictions away from well control.

It was particularly interesting that the workflow readily highlighted the recent Pyxis discovery at a stratigraphic level in which no other discoveries in the region had been identified.

The project shows that significant uplift is available by applying state-of-the-art technology to historic data. It also shows that working in partnerships, building flexible business models, and undertaking proactive technology-focused studies is highly effective in a constrained commercial environment. **TLE**

References

Department of Industry Tourism and Resources (DITR), 2007, 2007 offshore petroleum acreage release, CD.

Jablonski, D., and A. J. Saitta, 2004, Permian to Lower Cretaceous plate tectonics and its impact on the tectono-stratigraphic development of the Western Australian margin: APPEA Journal, **44**, no. 1, 287–327.

Kemper, M., and J. Gunning, 2014, Joint impedance and facies inversion — Seismic inversion redefined: First Break, **32**, no. 9, 89–95.

Longley, I. M., C. Buessenschuett, L. Clydsdale, C. J. Cubitt, R. C. Davis, M. K. Johnson, N. M. Marshall, A. P. Murray, R. Somerville, T. B. Spry, and N. B. Thompson, 2002, The North West Shelf of Australia — A Woodside perspective, *in* M. Keep, and S. J. Moss, eds., The sedimentary basins of Western Australia 3: Proceedings of the Petroleum Exploration Society of Australia Symposium, 27–88.

Editor's note: RokDoc Ji-Fi is a registered trademark of Ikon Science.